

PAPER • OPEN ACCESS

## Development of low inductance circuit for radially symmetric circuit

To cite this article: T Takayanagi *et al* 2019 *J. Phys.: Conf. Ser.* **1350** 012183

View the [article online](#) for updates and enhancements.

### You may also like

- [Thesaurus tool for analysing the semantic compatibility of educational texts](#)  
G R Rybakova, A Yu Andreeva, I V Krotova *et al.*
- [Investigations on the Stability of a Two-Wheeled Vehicle with a Tendency to Topple Sideways](#)  
R Sidharth, V K Pranav, G Nitheesh Kumar *et al.*
- [Corrigendum: Tensor Computations of Stochastic Dynamic Fields \(2021 Journal of Physics: Conference Series \(JPCS\), Vol. 1828, 012038\)](#)  
Yinsheng Zhang



**ECS** 244<sup>th</sup> Electrochemical Society Meeting

October 8 – 12, 2023 • Gothenburg, Sweden

50 symposia in electrochemistry & solid state science

▶ Deadline Extended!  
**Last chance to submit!**

New deadline:  
April 21  
**submit your abstract!**

# Development of low inductance circuit for radially symmetric circuit

T Takayanagi<sup>†</sup>, T Ueno and K Horino

<sup>†</sup>J-PARC/JAEA, 319-1195, Tokai-mura, Japan

E-mail: tomohiro.takayanagi@j-parc.jp

**Abstract.** The switch of the radially-symmetric circuit using semiconductors of SiC-MOSFET, which is one of the next-generation semiconductors, consists of a circuit in which many semiconductor switches are arrayed in parallel. Since all parallel circuits are equal in length, distortion due to timing jitter or impedance difference does not occur on principle in the merged output waveform. This circuit is useful for outputting an ultrashort pulse waveform. Therefore, we have developed a circuit board that achieves even lower inductance of the power transmission circuit by making a double ring structure equivalent to a coaxial shape. We compare the results of calculation, analysis and measurement, and the superiority of the developed coaxial-type is presented here.

## 1. Introduction

As a high-speed switch for high current and high voltage, many apparatuses adopt a thyatron switch [1]. The thyatron is the only device capable of switching a high current of multi-kiloampere in nanoseconds. However, since the thyatron is a discharge tube type, it requires several days of conditioning before it is used in operation in order to stabilize the internal plasma state. In addition, an unstable state in which the jitter becomes large may occur suddenly, or an event of sudden end of life may sometimes occur.

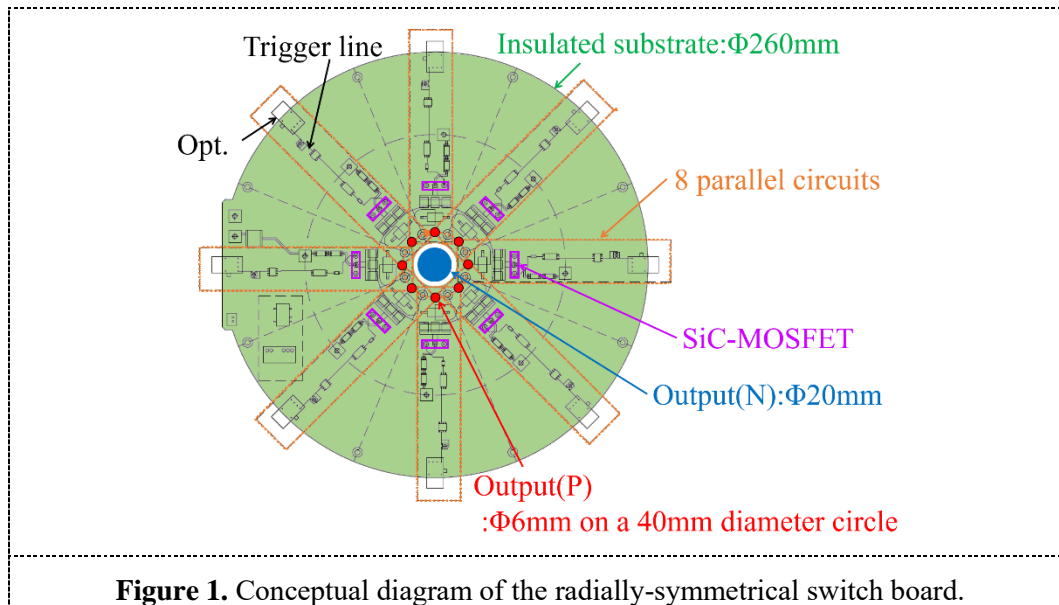
High-intensity proton beam accelerators such as J-PARC [2] require a kicker system [3] that excites a high-current, high-voltage output with an ultrashort pulse in order to extract a fast accelerated high-intensity beam. And, the current kicker system uses the thyatron. High speed switches require high performance with stable repeatability and setting accuracy. Therefore, we have developed a radially symmetric modular switch using SiC-MOSFET [4], which is one of the next generation semiconductors. The radially-symmetrical switch is composed of a parallel circuit in which many semiconductor switches are radially aligned in order to output a high current. The length of each parallel circuit is equal, and as a result, no jitter of operation timing or a difference in circuit impedance occurs, so it was confirmed by a test that distortion is not generated as compared with an output waveform by a general line-symmetrical circuit.

In order to put this radially-symmetrical switch into practical use as an alternative to thyatron switches, we proposed a structure to realize further reduction of the transmission line impedance. And the effectiveness was confirmed in the demonstration test using test circuit boards.

## 2. Circuit path design

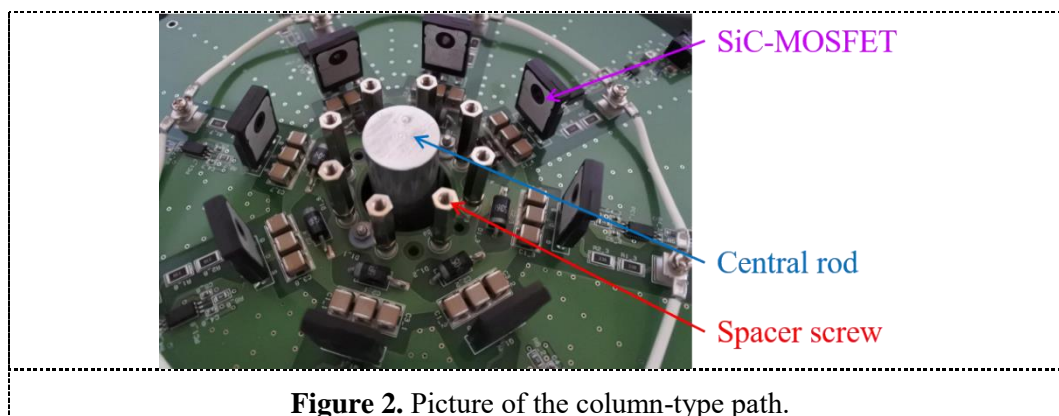


The test circuit board of the radially-symmetrical switch is composed of 8 parallel circuits [4]. In the case of outputting a higher voltage, the output voltage can be increased by stacking the circuit boards in multiple stages in series. In this test, two circuit boards with 800 V output per circuit board are stacked. A conceptual diagram of the board is shown in Fig. 1.



### 2.1. Basic structure

The current path between the stacked circuit boards is formed by connecting the 8 output (P) terminals using the cylindrical spacer screws as in the case of the LTD circuit [5]. This structure of the current path is called a “column-type” in this paper. A 6 mm diameter spacer screw is placed on a 40 mm diameter circle. There is a 28 mm round hole in the center of the board, and an output (N) terminal using a 20 mm diameter rod is inserted to form a current path for the return current. The picture of the column-type board is shown in Fig. 2.



### 2.2. Improved current path structure

Instead of the spacer screws, a cylindrical copper ring is used as current path between stacked circuit boards. The combination of the cylindrical ring and the central rod has the same structure as the coaxial cable in which the outer conductor surrounds the central conductor. In this paper, this structure

is called a “coaxial-type”. Such a coaxial structure can efficiently transmit high frequency pulses by the shielding effect that blocks the leakage of signals to the outside. Therefore, further reduction in inductance can be expected. Moreover, this structure can also suppress the influence of noise. Furthermore, there is an advantage that the design of the circuit system is easy because the characteristic impedance is constant. A picture of this circuit board with the coaxial-type is shown in Fig. 3

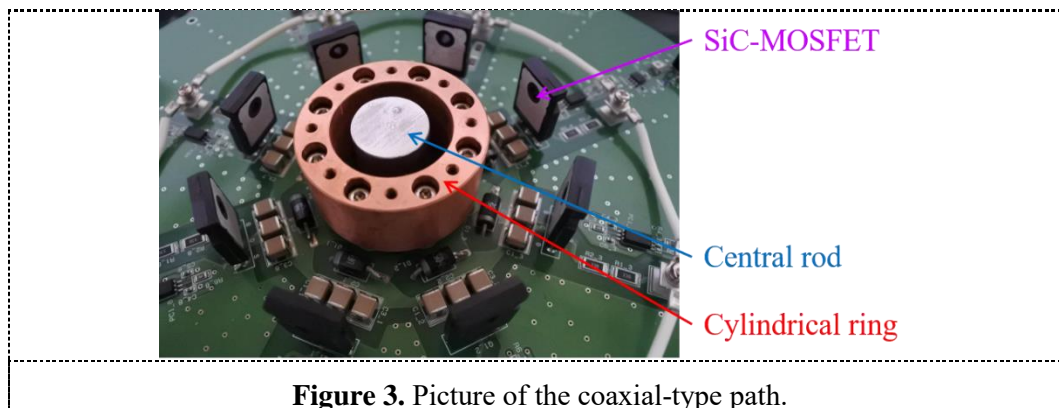


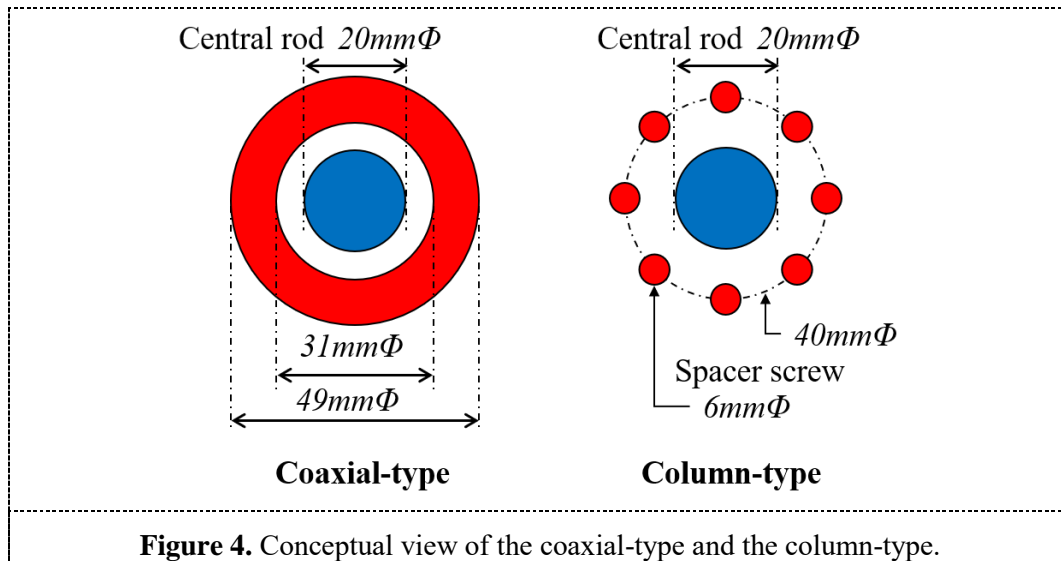
**Figure 3.** Picture of the coaxial-type path.

### 3. Inductance calculation

A conceptual view of the coaxial-type and the column-type is shown in Fig. 4. In the coaxial-type, the radius (a) of the inner conductor is 10 mm, the inner radius of the outer conductor (b) is 15.5 mm, and the outer radius (c) is 24.5 mm. There is an air layer between the inner and outer conductors. The self-inductance per unit length of the coaxial line can be obtained from Eq. (1). However, in the current output circuit, it is necessary to regard the transfer circuit as two coils and to evaluate the total inductance due to the structure of the circuit board. The total inductance can be estimated by the magnetic storage energy from the current flowing in the current path. Although this circuit is a pulse circuit, it was calculated using the static magnetic field two-dimensional analysis model using OPERA [6, 7] for reference. The contour maps of the magnetic flux density (B) of the two models analysed with OPERA-2D are shown in Fig. 5 and 6. It can be confirmed that the coaxial type has a well-rounded magnetic field distribution with less disturbance.

The self-inductance using the magnetic flux between the inner and outer conductors analysed by OPERA-2D is obtained from Eq. (2). The calculation results of the self-inductance at a current (I) of 400 A are shown in Table 1. The results of the Eq. (1) and the result using the analysis result of the Eq. (2) are nearly equal, indicating that the analytical model is correct.

The total inductance using the magnetic energy (We) is obtained from Eq. (3). The magnetic energy of the coaxial-type and the column-type analysed by OPERA-2D is 14.0 mJ/m and 15.1 mJ/m, respectively. So, the total inductances are 175.4 nH/m and 188.7 nH/m. The results are additionally shown in Table 1. The total inductance of the coaxial-type was reduced by about 10 % compared to the column-type.



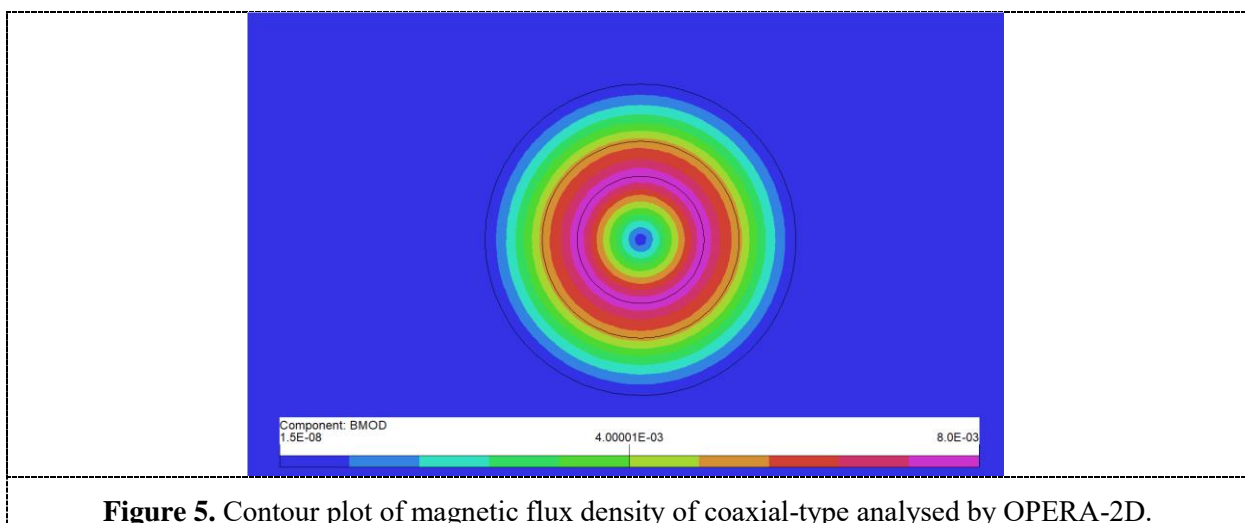
$$L = \frac{\mu_0}{2\pi} \ln \frac{b}{a} \quad [H/m] \tag{1}$$

$$L = \frac{\Phi}{I} \quad [H/m] \tag{2}$$

$$L = \frac{2W_e}{I^2} \quad [H/m] \tag{3}$$

**Table 1.** Calculated inductance

Path type	(1)	(2)	(3)
Coaxial	87.7nH/m	87.5nH/m	175.4nH/m
Column	-	113.3nH/m	188.7nH/m



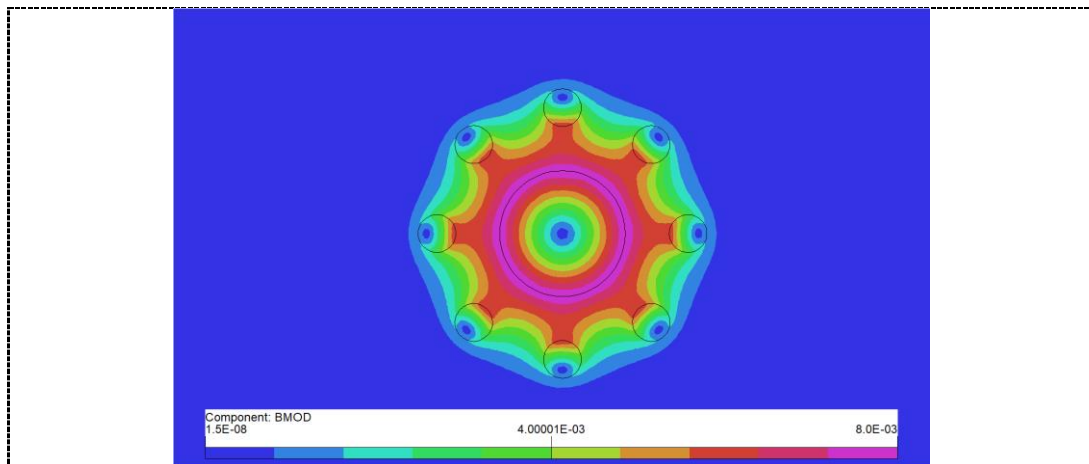


**Figure 6.** Contour plot of magnetic flux density of column-type analysed by OPERA-2D.

## 4. Measurement Result

### 4.1. Semiconductor switch operation test

The device of SiC-MOSFET is SCT3030KL made by Rohm Co., Ltd. The rated drain current  $I_D$  per element is 72 A. The circuit boards were stacked in two stages, and a  $3.75 \Omega$  load was connected to the output end. The circuit supplies 426.6 A at a charging voltage of 800 V. The result of measuring two types of output voltage waveforms is shown in Fig. 7. However, no difference was found between the two results. In this experiment using a semiconductor switch, the contribution of the inductance reduction is not visible because the loss is large.

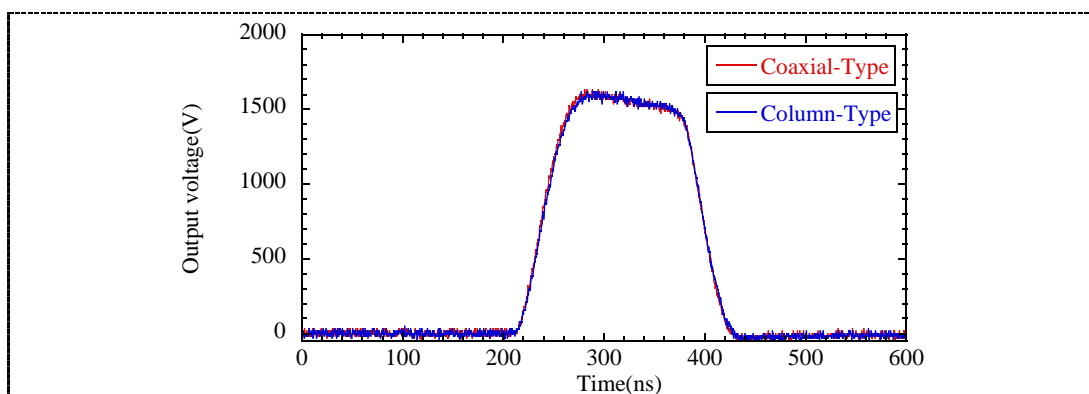


**Figure 7.** Measurement result of measuring two types of output voltage waveforms.

### 4.2. Gap switch test

Another test was performed using a gap switch. In this test, the FET switch was replaced by a gap switch at the output and all FET switches on the circuit are bypassed. In addition, all diode resistors were removed as shown in Fig. 8. By the setup, the inductance dependence of the current path structure can clearly be seen. A picture of the gap switch section is shown in Fig. 9.

After charging 40 V, the current waveform flowing through the central rod when the gap switch was short-ed was measured using a Rogowski coil (CWT Mini 30). The measured current



waveform is shown in Fig. 10, and the peak current and oscillation time obtained from the waveform are shown in Table 2. In the coaxial-type, the output current is 1.2 times higher and the oscillation time is 0.96 times shorter. The difference between the analysis and the experiment is the difference between static calculation and dynamic experiment. The analysis of the pulse circuit requires dynamic analysis including skin effect. In the future work, we evaluate the inductance dependence using the dynamic analysis of OPERA-3D [8].

The experimental test demonstrates the realization of low inductance with the improvement of the current path. It has been confirmed that the coaxial-type is superior for high speed pulse output waveforms.

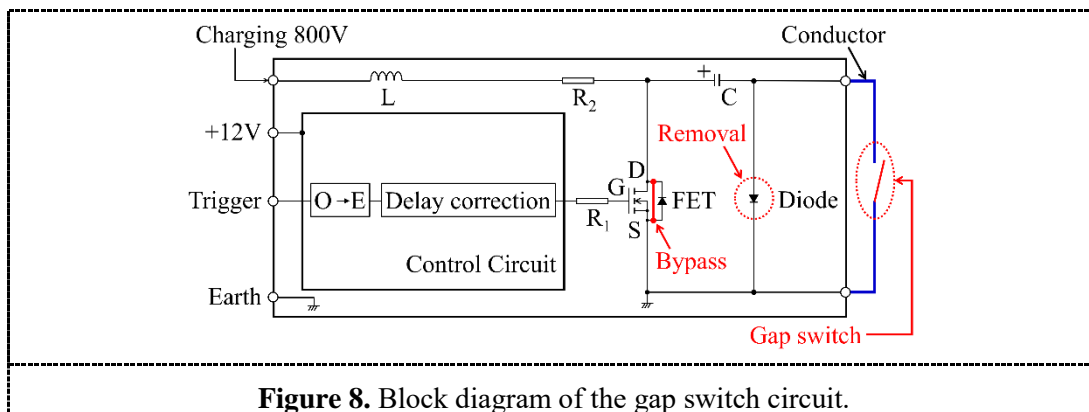


Figure 8. Block diagram of the gap switch circuit.

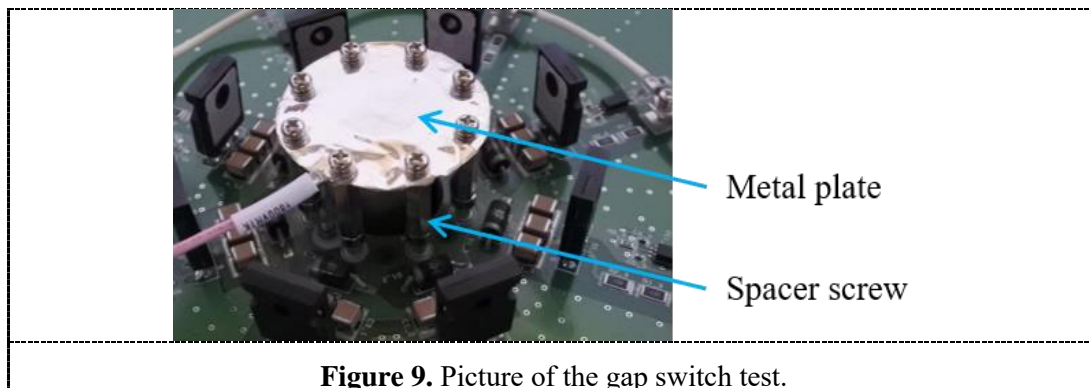


Figure 9. Picture of the gap switch test.

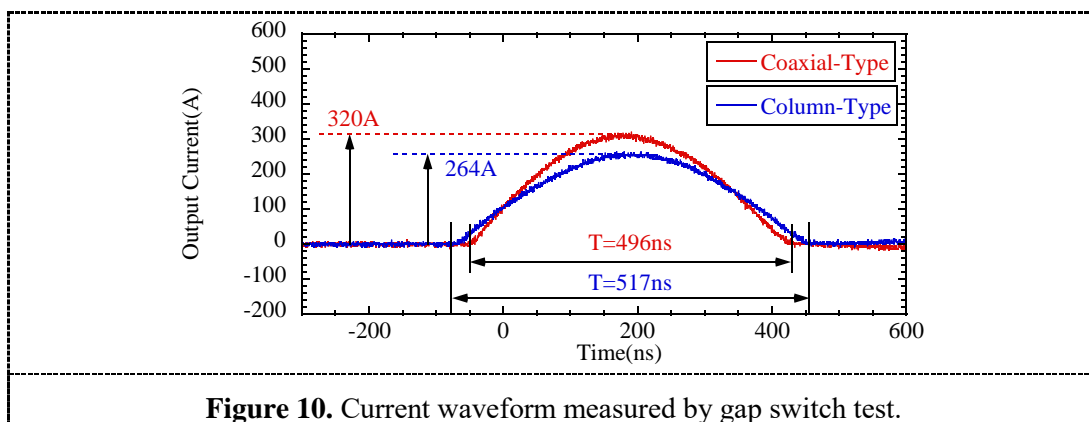


Figure 10. Current waveform measured by gap switch test.

**Table 2.** Experimental results

Path type	Peak current (A)	Period (s)
Coaxial	320	4.96E-07
Column	264	5.17E-07

## 5. Summary

The experimental results confirm that the coaxial-type can realize low inductance. Although the reduction rate of the inductance confirmed by the experiment results was about 10 %, this is a big effect in the output system of high-current, high-voltage, high-speed pulse waveforms. In the future, when a low impedance characteristic is required at the output stage with a large number of stacked layers, the coaxial path structure will be useful.

## Acknowledgements

This work was supported by JSPS KAKENHI Grant Number JP17K06334. The authors would like to thank A. Tokuchi and Y. Mushibe (Pulse Power Japan) for their technical support, and thank M. Kinsho, K. Yamamoto and Y. Irie for their participation in fruitful discussions and continuous support.

## References

- [1] Inagaki T *et al.*, “Development of a solid-state pulse generator driving kicker magnets for a novel injection system of a low emittance storage ring”, in *Proc. IPAC’18*, Vancouver, BC, Canada, May 2018, pp. 1804-07.
- [2] <https://j-parc.jp/index-e.html>
- [3] Kamiya J *et al.*, “Magnetic Field Mapping and Excitation Test in Vacuum for the Kicker Magnet in J-PARC RCS”, in *IEEE Trans. Appl. Supercond.*, vol. **18**, no. 2, June 2008, pp.293-6.
- [4] Takayanagi T *et al.*, “Development of a new modular switch using a next-generation semiconductor”, in *Proc. IPAC’18*, Vancouver, BC, Canada, May 2018, pp. 3841-44.
- [5] Jiang W *et al.*, “Pulsed Power Generation by Solid-State LTD”, in *IEEE Trans. on Plasma Science*, vol.42, no. 11, Nov. 2014, pp.3603-08.
- [6] <https://operafea.com/>
- [7] Takayanagi T *et al.*, “Simulation Model for Design of a New Power Supply”, in *IEEE Trans. Appl. Supercond.*, vol. **22**, no. 3, June 2012, pp.5400704.
- [8] Takayanagi T *et al.*, “A New Pulse Magnet for the RCS Injection Shift Bump Magnet at J-PARC”, in *IEEE Trans. Appl. Supercond.*, vol. **28**, no. 3, June 2018, pp.4100505